ELSEVIER

Biophysical Chemistry 73 (1998) 85–107

Biophysical Chemistry

Dynamic model of hormonal systems coupled by negative feedback

Casey H. Londergan, Enrique Peacock-López*

Department of Chemistry, Williams College, Williamstown, MA 01267, USA

Received 9 October 1997; received in revised form 20 February 1998; accepted 20 February 1998

Abstract

Most hormone concentrations in the body are regulated by negative feedback mechanisms in which the production and release of hormones are regulated according to the concentration of related species. Also, it has been observed that several hormones are released in a variety of pulsatile patterns. In most cases, the mechanism driving these complex patterns is not well understood. Our model of two cells coupled through negative feedback to their external products demonstrates periodic, aperiodic and chaotic oscillations. The coupling between the cells seems to be responsible for these dynamic behaviors. The variety of dynamic behaviors observed in the model demonstrates that a simple physiological feedback loop mimicking the coupling between circulatory hormones and production centers could be the source of complex hormone release patterns observed in vivo.

Keywords: Hormonal systems; Negative feedback coupling; Attractor coexistence; Quasaiperiodicity; Chaos

1. Introduction

Hormones are the chemical messengers in the body that play crucial roles in regulating many essential biochemical and physiological processes. The production and release of hormones and chemical messengers in the body are strictly regulated by feedback mechanisms. These mechanisms generally involve an element of negative feedback. The simplest negative feedback system involves a species' concentration directly influencing its own production. A more complicated and widely documented [1–10] form of negative feedback is a species concentration influencing the hormone that stimulates the species' production.

As in the case of a number of biological systems [11], oscillations in hormone concentration

* Corresponding author. Tel.: +1 413 5972434; fax: +1 413 5974116.

0301-4622/98/$19.00
PII S0301-4622(98)00140-9

are more the rule than the exception [12]. It has been postulated [13] and determined theoretically that periodic hormone release is actually the most efficient method of intercellular communication [14]. The underlying mechanisms leading to these periodic behaviors remain unknown, even in many experimentally documented systems.

The actual existence of deterministic phenomena, such as limit cycles and chaos in physiological systems, is a matter of debate; observation of oscillatory and possibly hyperchaos in physiological systems has revealed what could be pervasive in mammalian physiology [15]. Some physiological systems in which more complex dynamic behaviors have been observed are the heart, the brain, and the endocrine system. For many physiological systems a great deal needs to be understood about not just the mechanisms, but also the relative soundness of mathematical descriptions of different rhythmic physiological systems. Insights into states that are found naturally can be very helpful for both biology and medicine. Whether a system as simple as a two-cell feedback loop is capable of sustaining oscillations and other complicated release patterns is an issue that this paper addresses.

Since many hormonal systems operate in a pulsatile manner, the first prerequisite of any model is that it demonstrates the diverse oscillations observed in hormone systems. Also, many oscillating models are externally driven at a predetermined frequency. An external forcing rhythm of this type is not present in many physiological systems that exhibit oscillatory behavior. Formulating a model which, like physiological systems, will oscillate without an external forcing element is important in the modelling of oscillating physiological systems.

The significance of the coexistence of two attractors in models given the same biological machinery can not be underestimated. In an organism, hysteresis can be equated with the coexistence of a healthy temporal pattern and an unhealthy pattern in exactly the same organism or system under the same conditions. Given what can be considered a small perturbation, a productive or healthy temporal pattern can become unproductive or unhealthy. Examples of hysteresis or near-hysteresis between healthy and unhealthy physiological attractors have been documented in cardiac rhythms and brain waves. In cardiac rhythms, a heart attack represents a transition from a pulsatile state to an aperiodic high frequency state. Also, in brain waves during an epileptic seizure, a chaotic state suddenly becomes tightly periodic [15]. As mentioned above, it is believed that hormonal release patterns are most efficient if they are periodic; therefore it is not inconceivable that a healthy state's hysteresis with a non-periodic or less efficient state could lead to hormone-related disorders.

Hysteresis in models like our two-cell model below is present when two attractors coexist in phase space for the same parameter values. The attractor which a trajectory is drawn to depends entirely on the initial conditions. Models that exhibit hysteresis can be useful in predicting the degree and type of perturbation needed to force a physiological system from a 'healthy' attractor into another 'unhealthy' attractor.

In this paper, we propose a model to study mutual regulation between two production centers. The two centers are coupled through a mechanism of mutual feedback. The type of physiological system which the model emulates is a circulatory feedback loop, in which two centers of different hormones or chemical messengers are linked to each other by the concentration of the other center's product. In the body, the medium through which external concentrations move between cells and organs is the circulatory system. It is a matter of conjecture whether a system as simple as a circulatory feedback loop can be primarily responsible for the range of periodic behaviors observed in hormone concentrations in the body [8]. The two-cell model can be related to several types of feedback loops with a simple common distinction: all feedback loops which can be compared to the model must contain two external concentrations whose production and release are linked through negative feedback mechanisms. In Section 2, we introduce our two-cell model followed by numerical analysis in Section 3, and discussion of the implication of our results in Section 4.

2. Model of mutual regulation

The model considered in our work is a simple system of two coupled cells, which is depicted in Fig. 1. The cells are coupled to each other by a feedback mechanism in which the input of each cell is dependent on the concentration of the output of the other cell. Internally, each cell is a Higgins oscillator. The Higgins oscillator has been shown to exhibit a period-two limit cycle over a wide range of parameter values when its input is coupled to its own product [16]. The reaction steps of the Higgins oscillators proceed as follows. In each cell, the input of the first internal species, X or W, is regulated by the input function $f([U])$ or $f([Z])$,

$$X_{\text{external}} \overset{f([U])}{\rightarrow} X_{\text{internal}} \tag{1}$$

$$W_{\text{external}} \overset{f([Z])}{\rightarrow} W_{\text{internal}} \tag{2}$$

Next, X (W) is enzymatically transformed into a second internal species, $Y(V)$,

$$X + E_1 \overset{k^+_{1,1}}{\rightarrow} XE_1 \tag{3}$$

$$XE_1 \overset{k^+_{1,1}}{\rightarrow} X + E_1 \tag{4}$$

$$XE_1 \overset{k_{1,2}}{\rightarrow} Y + E_1 \tag{5}$$

$$W + E_3 \overset{k^+_{1,2}}{\rightarrow} WE_3 \tag{6}$$

$$WE_3 \overset{k^-_{2,1}}{\rightarrow} W + E_3 \tag{7}$$

$$WE_3 \overset{k_{2,2}}{\rightarrow} V + E_3. \tag{8}$$

The enzyme catalyzing the formation of Y (V) is activated by the presence of its product,

$$Y + \overline{E}_1 \overset{k^+_{a1}}{\rightarrow} E_1 \tag{9}$$

$$E_1 \overset{k^-_{a1}}{\rightarrow} Y + \overline{E}_1 \tag{10}$$

$$V + \overline{E}_3 \overset{k^+_{a2}}{\rightarrow} E_3 \tag{11}$$

$$E_3 \overset{k^-_{a2}}{\rightarrow} V + \overline{E}_3 \tag{12}$$

In the second enzymatic reaction, the second internal species, Y, is transformed into the final product, $Z(U)$, and released from the cell,

$$Y + E_2 \overset{k^+_{1,3}}{\rightarrow} YE_2 \tag{13}$$

$$YE_2 \overset{k^-_{1,3}}{\rightarrow} Y + E_2 \tag{14}$$

$$YE_2 \overset{k_{1,4}}{\rightarrow} Z + E_2 \tag{15}$$

$$V + E_4 \overset{k^+_{2,3}}{\rightarrow} VE_4 \tag{16}$$

$$VE_4 \overset{k^-_{2,3}}{\rightarrow} V + E_4 \tag{17}$$

$$VE_4 \overset{k_{2,4}}{\rightarrow} U + E_4 \tag{18}$$

The concentration of both external products Z and U decays at a given rate,

$$Z \overset{k_{d1}}{\rightarrow} \phi \tag{19}$$

$$U \overset{k_{d2}}{\rightarrow} \phi \tag{20}$$

Assuming steady states for all of the enzymes and enzyme complexes, this reaction scheme can be simplified to the following reactions:

$$X_0 \overset{k_{0,1}f(U)}{\rightarrow} X \tag{21}$$

$$X + Y \overset{k_{1,1}}{\rightarrow} 2Y \tag{22}$$

$$Y \overset{E}{\rightarrow} Z \tag{23}$$

$$Z \overset{d_1}{\rightarrow} \phi \tag{24}$$

$$W_0 \overset{k_{0,2}f(Z)}{\rightarrow} W \tag{25}$$

$$W + V \overset{k_{1,2}}{\rightarrow} 2V \tag{26}$$

$$V \overset{E}{\rightarrow} U \tag{27}$$

$$U \overset{d_2}{\rightarrow} \phi \tag{28}$$

The mass action laws for each of the species in the simplified reaction scheme are the following:

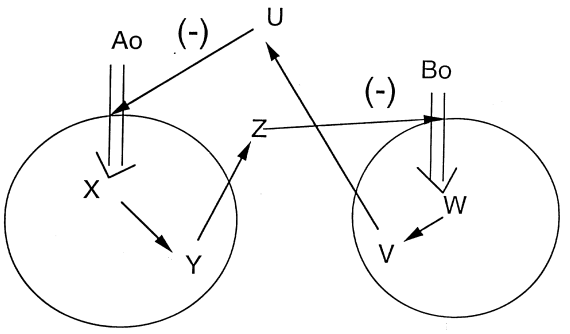

Fig. 1. Schematic diagram of the two-cell system.

$$\frac{d[X]}{dt} = k_{0,1}X_0 f([U];U_0,m_1) - k_{1,1}[X][Y] \quad (29)$$

$$\frac{d[Y]}{dt} = k_{1,1}[X][Y] - \frac{V_{m1}[Y]}{K_{M1}+[Y]} \quad (30)$$

$$\frac{d[Z]}{dt} = \frac{V_{m1}[Y]}{K_{M1}+[Y]} - d_1[Z] \quad (31)$$

$$\frac{d[W]}{dt} = k_{0,2}W_0 f([Z];Z_0,m_2) - k_{1,2}[W][V] \quad (32)$$

$$\frac{d[V]}{dt} = k_{1,2}[W][V] - \frac{V_{m2}[V]}{K_{M2}+[V]} \quad (33)$$

$$\frac{d[U]}{dt} = \frac{V_{m2}[V]}{K_{M2}+[V]} - d_1[U] \quad (34)$$

where now the input functions $f([U])$ and $f([Z])$ are specified to be $f([U];U_0,b_1)$ and $f([Z];Z_0b_2)$.

The functional form of these regulated inputs is given by:

$$f([J],J_0b) = \frac{1}{1+e^{b([J]-J_0)}} \quad (35)$$

The function in Eq. (35) ranges between a minimum value of zero, or no input, and a maximum value, or the full input allowed by the cell. This sigmoidal behavior has been observed in the percentage of open channels in the presence of an inhibitor. Thus, Eq. (35) models an on/off input response to an inhibitor.

For ease of analysis, time and concentrations are redefined as dimensionless quantities. In this case, the new dimensionless variables (x,y,z,w,v,u) and time (τ) relate to the original concentrations and time through the following scaling:

$$[X] = K_{M1}x \quad (36)$$

$$[Y] = K_{M1}y \quad (37)$$

$$[Z] = K_{M1}z \quad (38)$$

$$[W] = K_{M2}w \quad (39)$$

$$[V] = K_{M2}v \quad (40)$$

$$[U] = K_{M2}u \quad (41)$$

$$t = \frac{\tau}{k_{1,1}K_{M1}} \quad (42)$$

where we have considered $k_{1,2}\ K_{M2} = k_{1,1}\ K_{M1}$. With these dimensionless variables, the mass action laws for the oscillators' species (21)–(28) reduce to the following dimensionless ordinary differential equations (ODEs):

$$\frac{dx}{d\tau} = A_1\sigma_1 - xy \quad (43)$$

$$\frac{dy}{d\tau} = xy - \frac{q_1 y}{1+y} \quad (44)$$

$$\frac{dz}{d\tau} = \frac{q_1 y}{1+y} - k_1 z \quad (45)$$

$$\frac{dw}{d\tau} = A_2\sigma_2 - wv \quad (46)$$

$$\frac{dv}{d\tau} = wv - \frac{q_2 v}{1+v} \quad (47)$$

$$\frac{du}{d\tau} = \frac{q_2 v}{1+v} - k_2 u \quad (48)$$

where the following parameters are defined in terms of the original rate constants:

$$A_1 = \frac{X_0 k_{0,1}}{k_{1,1}K_{M1}^2} \quad (49)$$

$$q_1 = \frac{V_{m1}}{k_{1,1}K_{M1}^2} \quad (50)$$

$$k_1 = \frac{d_1}{k_{1,1} K_{M1}} \tag{51}$$

$$A_2 = \frac{W_0 k_{0,2}}{k_{1,2} K_{M2}^2} \tag{52}$$

$$q_2 = \frac{V_{m2}}{k_{1,2} K_{M2}^2} \tag{53}$$

$$k_2 = \frac{d_2}{k_{1,2} K_{M2}} \tag{54}$$

The input functions are redefined as follows

$$\sigma_1 = \frac{1}{1 + e^{b(u - u_0)}} \tag{55}$$

$$\sigma_2 = \frac{1}{1 + e^{c(z - z_0)}} \tag{56}$$

with the following parameters:

$$b = K_{2M} m_1 \tag{57}$$

$$u_0 = \frac{U_0}{K_{2M}} \tag{58}$$

$$c = K_{1M} m_2 \tag{59}$$

$$z_0 = \frac{Z_0}{K_{1M}} \tag{60}$$

The coupling functions (55) and (56) make the oscillators' inputs dependent on each other's outputs around a threshold concentration (u_0 or z_0). The sensitivity parameter b or c defines how abrupt a change takes place in the input in the region near the threshold concentration.

Coupled oscillator models have been used to model many different kinds of systems and range from just two coupled oscillators to larger collections of reactive centers [11]. Our model is different in that it allows for analysis of a system coupled by external concentrations and not by the typical diffusion coupling [17,18]. Also, our model can be related to a system of oscillators coupled at a short distance from each other and linked only by external chemical species. For this reason, it can be used in analyzing endocrinological systems as well as any other systems that are coupled at a distance and share only a common external medium.

Table 1
Parameters and physical analogs

Coupling parameters	
A_1, A_2	Maximum input allowed by input channels Number of input channels Efficiency of input
b, c	Sensitivity to threshold concentration Efficiency of open/closed mechanism
u_0, z_0	Upper threshold concentration
Non-coupling parameters	
q_1, q_2	Internal reaction rate
k_1, k_2	Decay rate of products

In the model, we have five pairs of parameters. These parameters can be related to different physical aspects of the negative feedback mechanism, and together the parameters contribute to what is a reasonably comprehensive model. The parameters can be related to the physical properties listed in Table 1. These properties can be generalized to fit a large variety of feedback loops with a range of mechanisms involved in coupling the input of an oscillator to an external concentration, including different types of regulated input channels in cell membranes and neuron-mediated mechanisms of feedback coupling. Our model is flexible in ways that reflect most of the physical properties of negative feedback. The simplest circulatory feedback loop is a center to center system, in which two self-contained biological centers produce an external product in response to the other center's external product. A very simple example of a system like this is the communication of two bacteria or cells through two different chemical concentrations. An example of this type of communication is the communication of phosphorescent bacteria with the cells in an undeveloped squid's light-producing organ [19]. In relation to this case, the model's centers would represent individual cells.

A larger-scale system of the model's type is the communication of two organ-based hormone or chemical production centers in which the model's oscillators are comparable to these production

centers. An even more global potential application of the model is a step up from single production centers to relating the model's oscillators to entire hormonal axes, or the whole multi-organ, multi-chemical processes involved in producing a given hormone or chemical messenger. Combinations of the cell, organ, and hormonal axis relations are not inconceivable systems which we could analyze using the model if we were able to make the appropriate adjustments in parameter values.

A system which lends itself to analysis with our model is the endocrinological communication system between the hypothalamus and the pituitary gland. The hypothalamus is a region of the brain which is located quite close to the pituitary gland. The pituitary gland is a hormone-releasing gland and plays a major role in almost every bodily process from growth to metabolism to sexual development. The main communication between different regions of the hypothalamus and pituitary gland is not through direct neuronal connections but through the release of hormones into the hypophyseal portal vessels. These vessels transport chemicals straight to the pituitary gland. Pituitary-produced species released into the bloodstream eventually feed back to the hypothalamus [7].

Although the communication through external concentration in the case of the hypothalamus/pituitary complex takes place on what is in practical terms a short, closed track the key chemical links are still made via the circulatory system. Modelling a system involving the production and mutual regulation through circulation of two linked hypothalamic and pituitary hormones is a main objective of our two-cell model.

3. Numerical results

Since the system of six differential Eqs. (43)–(48), cannot be solved analytically, the model's behavior was studied through numerical integration. Numerical integrations were performed to two different ends: construction of trajectories and bifurcation analyses [20,21]. Characterization of attractors whose maxima were observed on bifurcation diagrams involved studying trajectories in phase space via two- and three-dimensional projections of attractors. In our study, we have used the INSITE software package [22]. Initial numerical integrations were performed using PLOD version 6 [23]. In both cases, we used the Gear algorithm, with integration tolerances of 10^{-12} for PLOD and 10^{-14} for INSITE.

In previous work, we have demonstrated that single Higgins oscillators would sustain simple period-one oscillations over a rage of parameter values [16]. Thus the numerical integrations were initialized using parameter values from our previous work; the initial parameter values appear in Table 2. With these initial parameters as a reference, one member of each pair of parameters was adjusted at first to investigate which parameters would potentially have the greatest effect on the nature of the dynamical behavior of the system.

With all of the parameter pairs set equal to the reference values, a period-one state was observed. This behavior was expected based on the previous study of a single oscillator. Next, the parameters of one of the cells were varied from the reference values, and three pairs of coupling parameters were determined to have the greatest effect on the system's dynamic behavior. In very simple bifurcation analyses, we observed that the q and k parameter pairs only had the effect of slightly altering the period and amplitude of the period-one state observed at the reference values. In similar simple analyses in which a coupling parameter was varied, we observed that the coupling parameters had the effect of radically changing the dynamical behavior.

On the basis of the preliminary observations of the relative importance of the coupling parameters, a systematic approach was devised to explore

Table 2
Reference parameter values from Peacock-López and Patel [16]

Parameter	Value
A_1, A_2	6
b, c	3
u_0, z_0	10
q_1, q_2	8
k_1, k_2	1

the range of dynamical behavior in regions of parameter space close to the reference parameter values. The two non-coupling pairs of parameters were set slightly different so that the model would reflect a system of two distinct cells with distinct products. The parameter values which we set constant throughout the analysis are listed in Tables 3 and 4. The oscillator with the greater k value was assigned the smaller q value for the reason that a final species with a slower production rate and smaller rate constant q would more likely have a faster rate of decay and larger decay constant k.

The approach to exploring the parameter space around the reference values consisted of varying one of each of the three coupling parameter pairs over different sets of fixed values of the other coupling parameters. All varied parameters corresponded to input of the w–v–u oscillator. The combinations of the non-varied parameter pairs were based on a qualitative greater- or less-than scheme; each parameter was varied over four sets of parameter values.

3.1. Parameter dependence

3.1.1. Variation of A_2

The A parameters correspond to the degree of input and multiply the coupling functions. Variation in these parameters in the immediate vicinity of the reference values led to the observation of several different routes to chaos.

At the first set of parameter values, the external product's dynamics of the two oscillators were markedly different as we can see from Fig. 2a,b. Namely, the output z from the x–y–z oscillator remained at almost constant amplitude, while the output u from the other oscillator went through a period-doubling cascade to chaos. In this case, the period-one state of the x–y–z oscillator drives the second oscillator through a wide range of more complex behaviors. At the second set of parameter values, the bifurcation diagrams show coincident windows of periodicity and chaos. Also Fig. 3a,b depicts a route to chaos which is slightly different from the typical period-doubling route.

Since the oscillators' inputs dependent on the external products, reducing one of the As to zero halts the production of z or u and uncouples the cells. The behavior of the outputs as A_2 approaches zero is complex as this uncoupling sequence is initiated; this can be seen in Fig. 4. It is a pattern of alternating behaviors which appear towards $A_2 = 0$. Increasingly thin windows of periodicity and chaos alternate as the cells are uncoupled. This pattern near $A_2 \approx 0$ was observed in both cells' outputs over all parameter values when varying A_2 with small differences in the relative widths of the periodic and chaotic windows. Its appearance in both oscillators indicates that it is the only uncoupling pattern for the model and that once one cell becomes near-uncoupled, its output pattern dominates the dynamics of the system.

Varying A parameters above values of approx. 12 did not significantly change the behavior of the system. Large A values would be of questionable physical significance because they would impinge on the assumption in the model of an excess of starting material for the oscillators.

Table 3
Constant values of non-coupling parameters

Parameter	Set value
q_1	10
k_1	1
q_2	8
k_2	1.2

Table 4
Parameter values for all figures

$q_1 = 10$, $k_1 = 1$, $q_2 = 8$, $k_2 = 1.2$

Figure	A_1	A_2	b	c	u_0	z_0
2	6	Varied	5	1	10	5
3	6	Varied	5	1	5	10
4	6	Varied	1	5	5	10
5	7	5	5	Varied	5	10
6	7	5	5	1	5	Varied
7	7	5	1	5	5	Varied
8	7	5	5	1	5	4.3
9	7	5	1	5	5	12
10	7	5	1	5	5	Varied
11	6	Varied	5	1	10	5

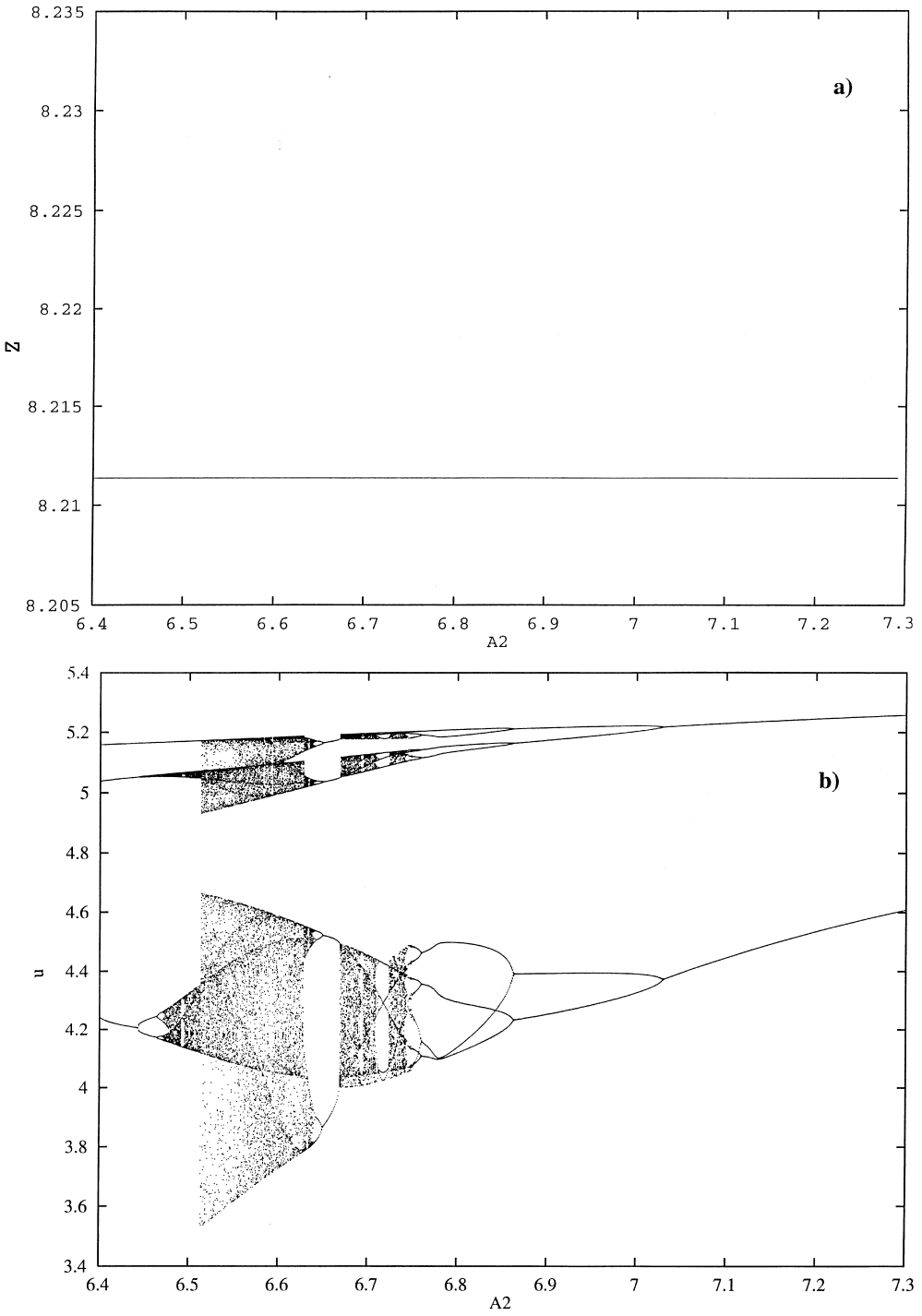

Fig. 2. Poincaré section defined by the local maxima of (a) z and (b) u varying A_2, with $u_0 = 10$ and $z_0 = 5$. Other parameters given in Table 4.

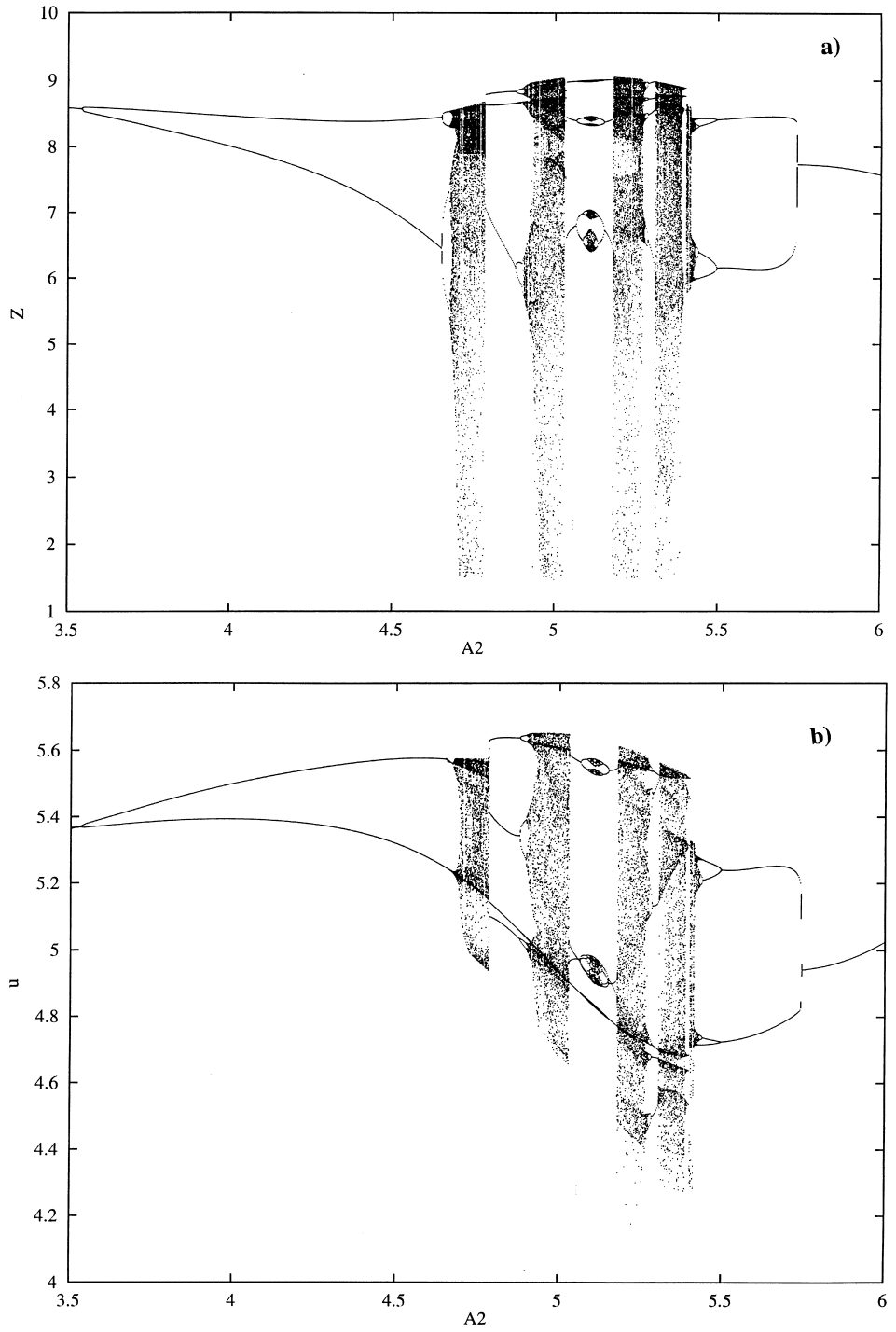

Fig. 3. Poincaré section defined by the local maxima of (a) z and (b) u varying A_2, with $b = 5$, $c = 1$, $u_0 = 5$ and $z_0 = 10$. Other parameters given in Table 4.

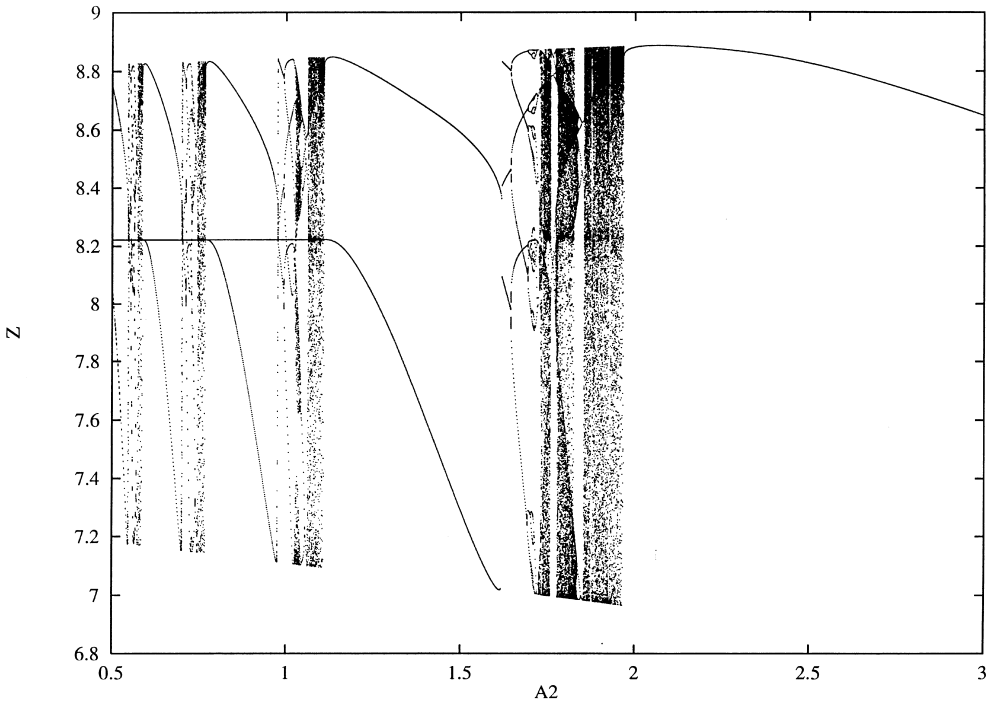

Fig. 4. Poincaré section defined by the local maxima of z varying A_2, with $b = 1$, $c = 5$, $u_0 = 5$ and $z_0 = 10$. Other parameters given in Table 4.

3.1.2. Variation of c

Varying values of c exhibited a range of behaviors, but not with the variability of behavior observed in varying A_2. For example, no bifurcations were observed above $c = 5$. From this it was concluded that $c = 5$ defines a steep enough input function that any value of c above five would be irrelevant to our analysis. Below $c = 1$ some bifurcations were observed, but the physical significance of b or c values less than one is questionable because of the lack of a definite opened/closed threshold. The variety of behavior with these constraints is best seen in Fig. 5a,b. It is interesting to note that in the case of Fig. 5a,b, period-doubling route to chaos is only observed for the x–y–z cell when c varies from unity to six.

3.1.3. Variation of z_0

Although complex behaviors were observed varying A_2 and c, the greatest variety of behaviors was observed while varying the threshold parameter z_0. Varying a threshold parameter was found to be the best way of looking at a wide range of dynamical behaviors over a relatively small region of parameter space.

When z_0 was varied towards zero, which makes the input of the second oscillator sensitive to traces of the first's product, a very complex sequence of bifurcations was observed. This observation could lead to a conclusion that the behavior of a negative feedback loop to trace amounts is different from a feedback loop which is sensitive only to concentrations near a threshold. An example of the type of bifurcation diagram observed varying z_0 is presented in Fig. 6a,c. A window of chaos is observed in both oscillators' outputs between $z_0 = 8$ and $z_0 = 10$. Above $z_0 = 18$ changes in dynamic behavior cease. In a more detailed bifurcation diagram, Fig. 6b, we can see the more fine structure of the bifurcation diagram corresponding to a homoclinic orbit.

Another illustration of the variety of complex dynamics is observed while varying z_0 as shown by Fig. 7a,b. The homoclinic orbit appears below

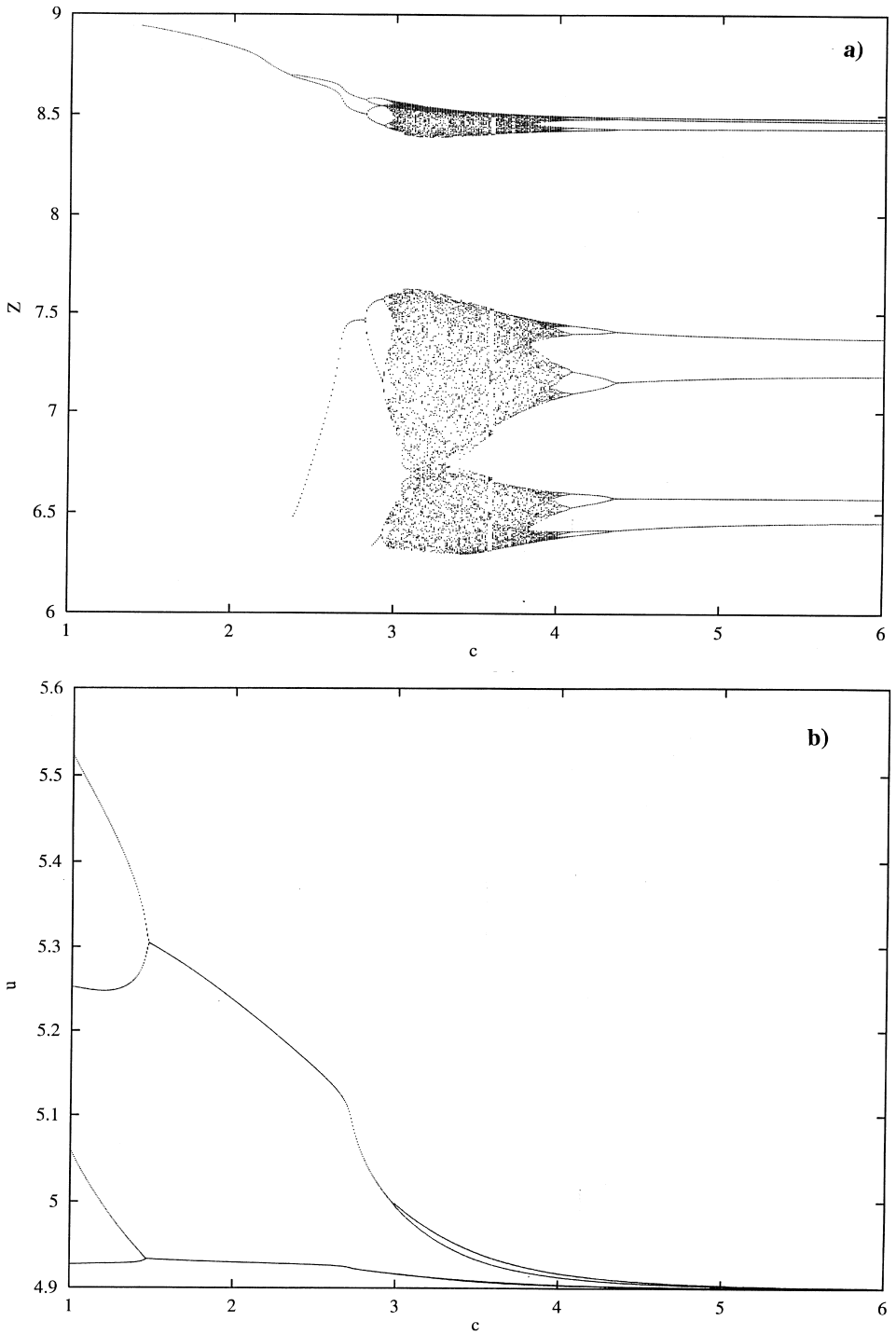

Fig. 5. Poincaré section defined by the local maxima of (a) z and (b) u varying c. Other parameters given in Table 4.

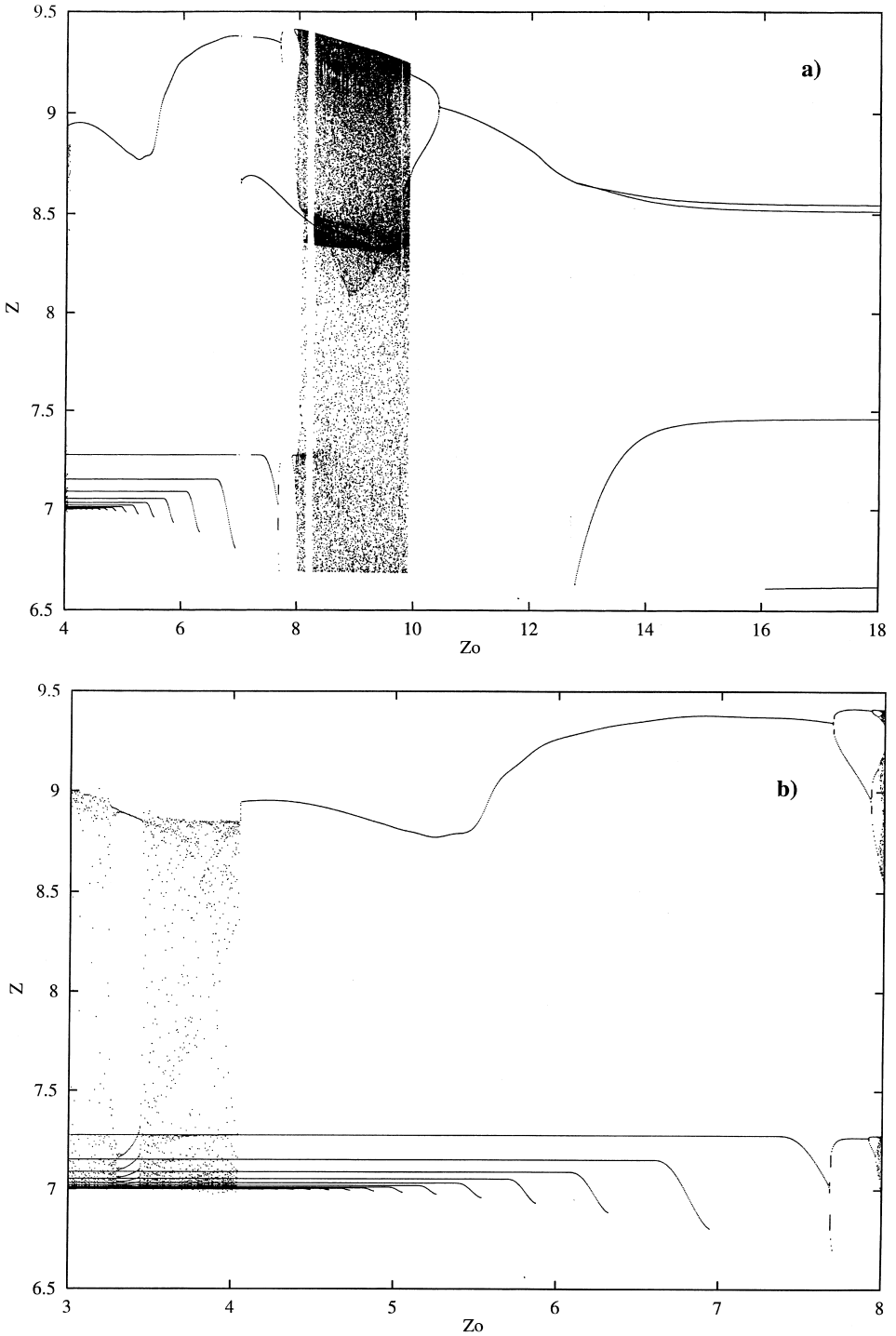

Fig. 6. Poincaré section defined by the local maxima of (a) z and (b) u varying z_0, with $A_1 = 7$, $A_2 = 5$, $b = 5$, $c = 1$. Other parameters given in Table 4.

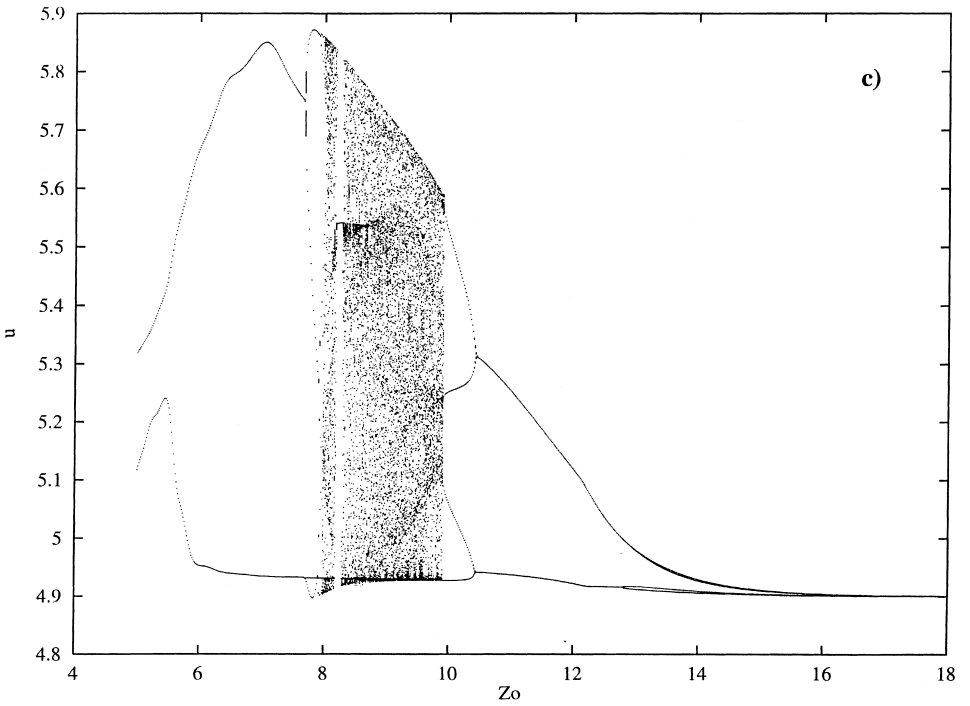

Fig. 6. (*Continued*)

$z_0 = 8$, and an attractor with many maxima is observed at all values above $z_0 = 11$. The latter attractor was shown to be the manifestation of a quasiperiodic trajectories. Also, series of period-doubling and other bifurcations which have yet to be fully characterized were observed between $z_0 = 9$ and $z_0 = 11$.

As outlined before, a large number of different types of dynamical behavior [20] were observed in bifurcation analyses varying coupling parameters. Finally, the most conspicuous behaviors were characterized using projections of trajectories in phase space at specific parameter values.

3.2. Complex dynamics

3.2.1. Homoclinic orbit

The pattern observed in Fig. 6a,c below $z_0 = 8$ was characterized using a projection of trajectories in the x–y–z space. One attractor, at $z_0 = 4.3$ is shown in Fig. 8a,c. In Fig. 8c, the location of the saddle point of the attractor is evident. By looking more closely at the saddle point (Fig. 8d), it became evident that the attractor represents a homoclinic orbit.

The Rössler-type slow manifold [24] or the Barkley scheme [25] are usually evoked to describe homoclinic orbits. The Rössler-type scheme is characterized by a very fast reinjection to the saddle-focus. Once within the slow manifold, the orbit spirals out. The Barkley scheme is characterized by a reinjection into the neighborhood of the saddle-focus. After reinjection, the orbit approaches the saddle-focus via damped oscillations. Also, the Barkley scheme allows long quiescent periods between damped oscillations and reinjection. The homoclinic orbits observed in our model seem to follow the Barkley scheme.

The appearance of the homoclinic orbit is significant to many conclusions that can be made about the model. The model can easily support complex dynamical behavior like the homoclinic orbit. The period of pulses in the time series associated with the homoclinic orbit is long com-

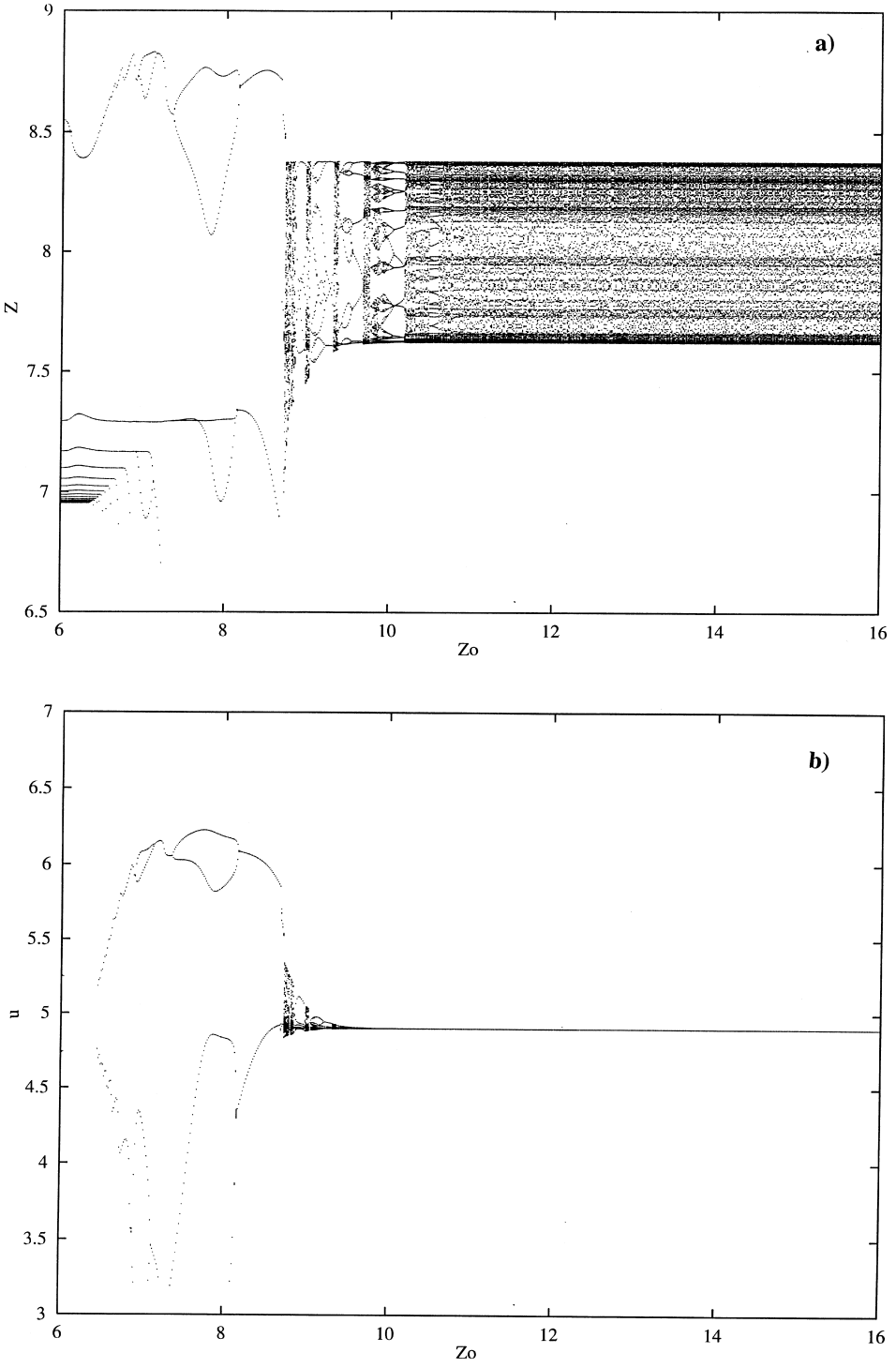

Fig. 7. Poincaré section defined by the local maxima of (a) z and (b) u varying z_0, with $A_1 = 7$, $A_2 = 5$, $b = 1$, $c = 5$. Other parameters given in Table 4.

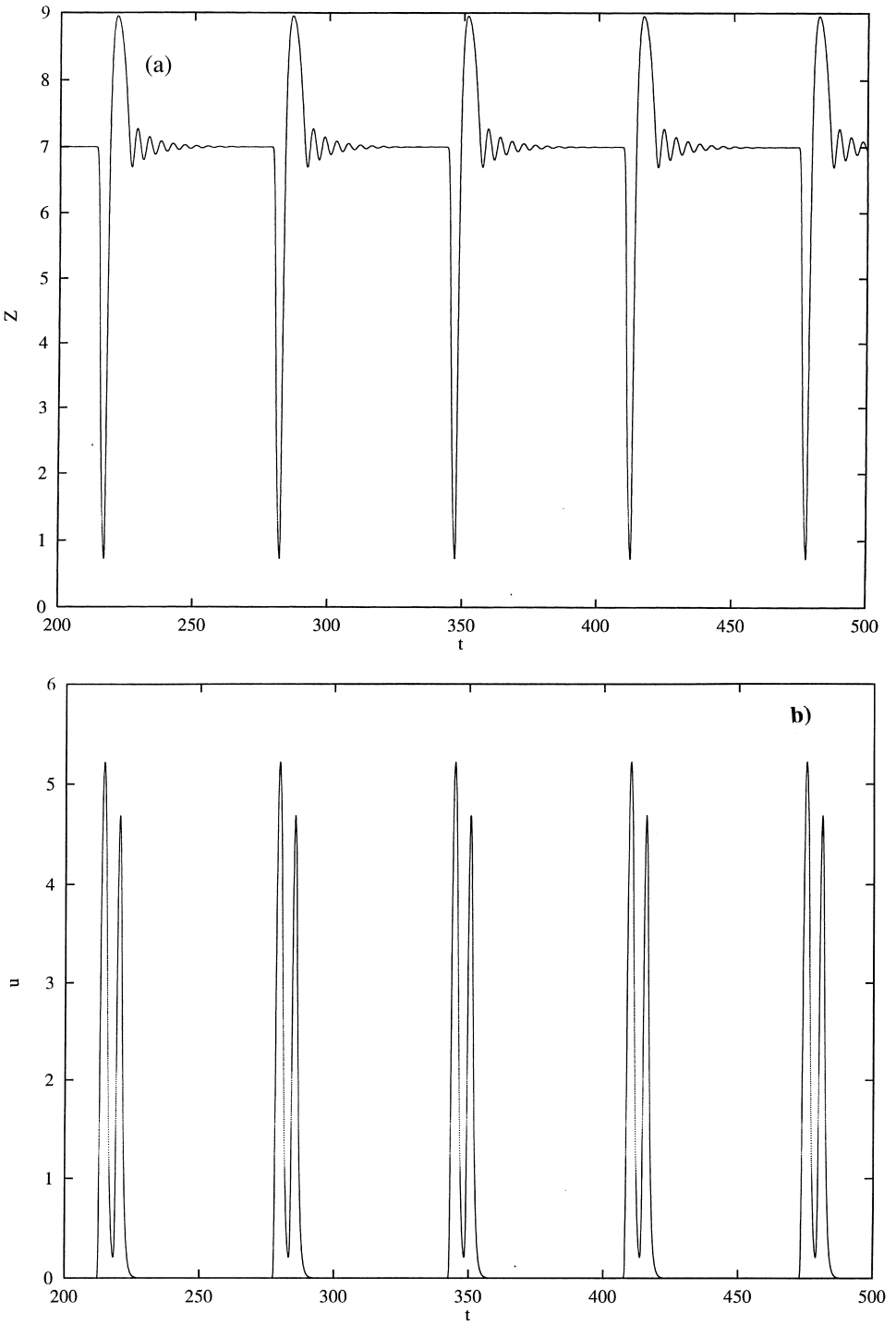

Fig. 8. Time series for (a) z and (b) u. (c) Three dimensional x–y–z phase space and (d) amplification. Parameters as in Fig. 7 with $z_0 = 4.30$

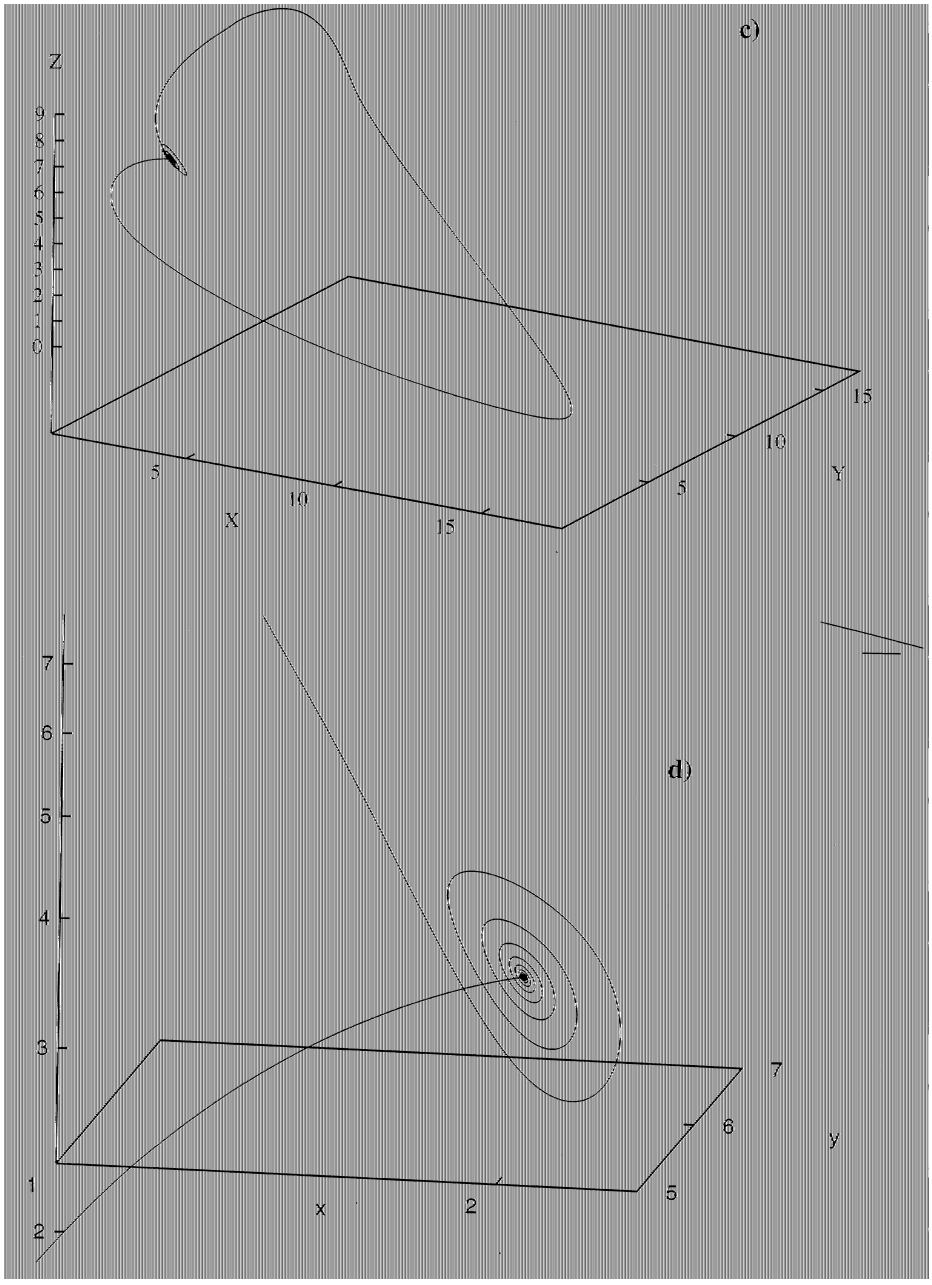

Fig. 8. (*Continued*)

pared to the typical periods of simpler periodic states. This fact could help to explain the exceedingly long periods seen in pulsatile release of some hormones. Finding that this type of behavior is inherent to our simple model makes it conceivable that it could appear in a more mechanistically complex but similar physiological system. Note that similar time series and homoclinic orbit attractors have been observed experimentally in an electrochemical system [26] and theo-

retically in a model of the peroxidase–oxidase reaction [27,28].

3.2.2. Quasiperiodicity

In Fig. 7a, the behavior, which exhibits almost no changes as z_0 is increased above 11, appeared on the bifurcation diagram and in the time series (Fig. 9a), to be chaotic. However, when the phase space projection (z–u–x), was constructed (Fig. 9b). The attractor appeared to be toroidal.

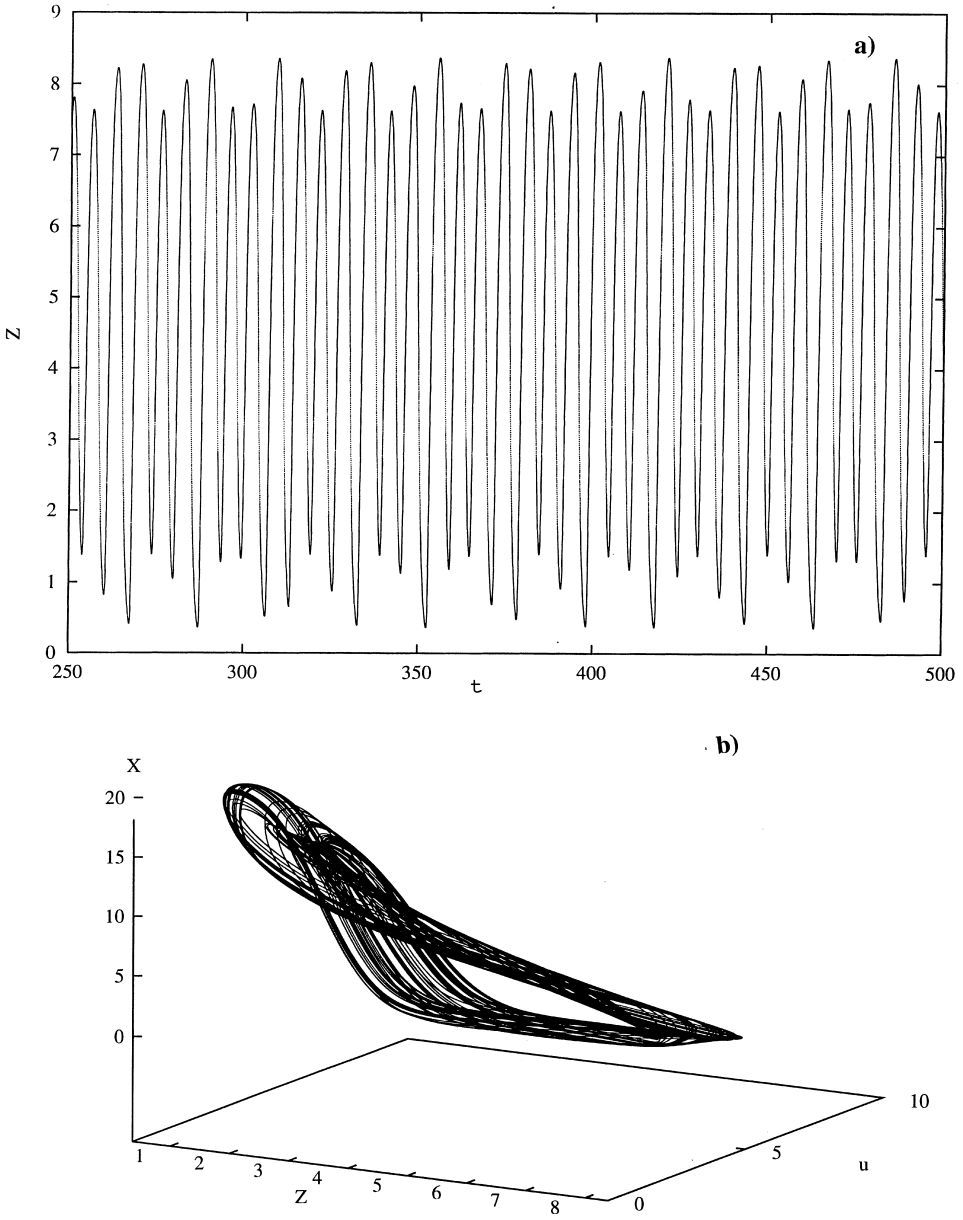

Fig. 9. (a) Time series for z. (b) Three-dimensional z–u–x phase space. (c) Next maximum map. Parameters as in Fig. 8 with $z_0 = 12.00$.

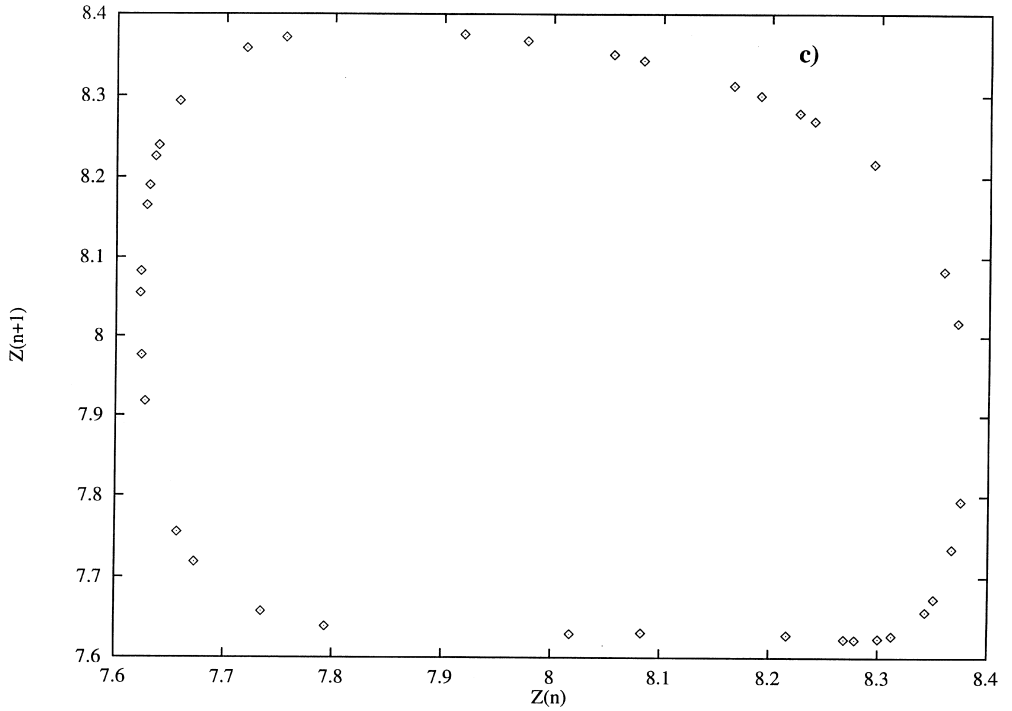

Fig. 9. (*Continued*)

Toroidal attractors are characteristic of quasiperiodicity. To confirm the toroidal nature of the behavior, a next maximum map of the maxima of z was constructed (Fig. 9c), and the circular toroidal cross-section observed confirmed the existence of quasiperiodicity.

Observation of quasiperiodicity in models is not a new phenomenon, but the appearance of quasiperiodicity in this model which does not possess an external forcing periodic term is interesting. Quasiperiodicity is most often observed when an external periodic driving term is present in a model and underlies any other periodic behavior that may occur. In our model, quasiperiodicity can be explained by realizing that while the output pattern for the x–y–z oscillator is complex, the output pattern of the w–v–u oscillator is periodic. The periodic release of the w–v–u oscillator is driving the quasiperiodic orbit.

Quasiperiodicity is another complex behavior which our model supports within itself. Observation of quasiperiodicity was further evidence that the simple model and similar physiological systems could be capable of sustaining complex dynamical behaviors.

3.2.3. Attractor coexistence

For several bifurcation analyses which proceeded forward and backward, we observed qualitatively different attractors for the same parameter values. An example of this birhythmicity was observed in the range of parameters of the homoclinic orbit. In Fig. 10a, which is comparable with Fig. 7a, we observed an attractor exhibiting a more typical period-doubling route to chaos coexisting with a homoclinic orbit. In Fig. 10b, we constructed both attractors for $A_2 = 6.08$; the two attractors lie just alongside each other in phase space. In Fig. 10c we show the region near the saddle point.

Another example of hysteresis is observed in Fig. 11a when it is compared to the non-backtracked diagram in Fig. 2b. In this case, two

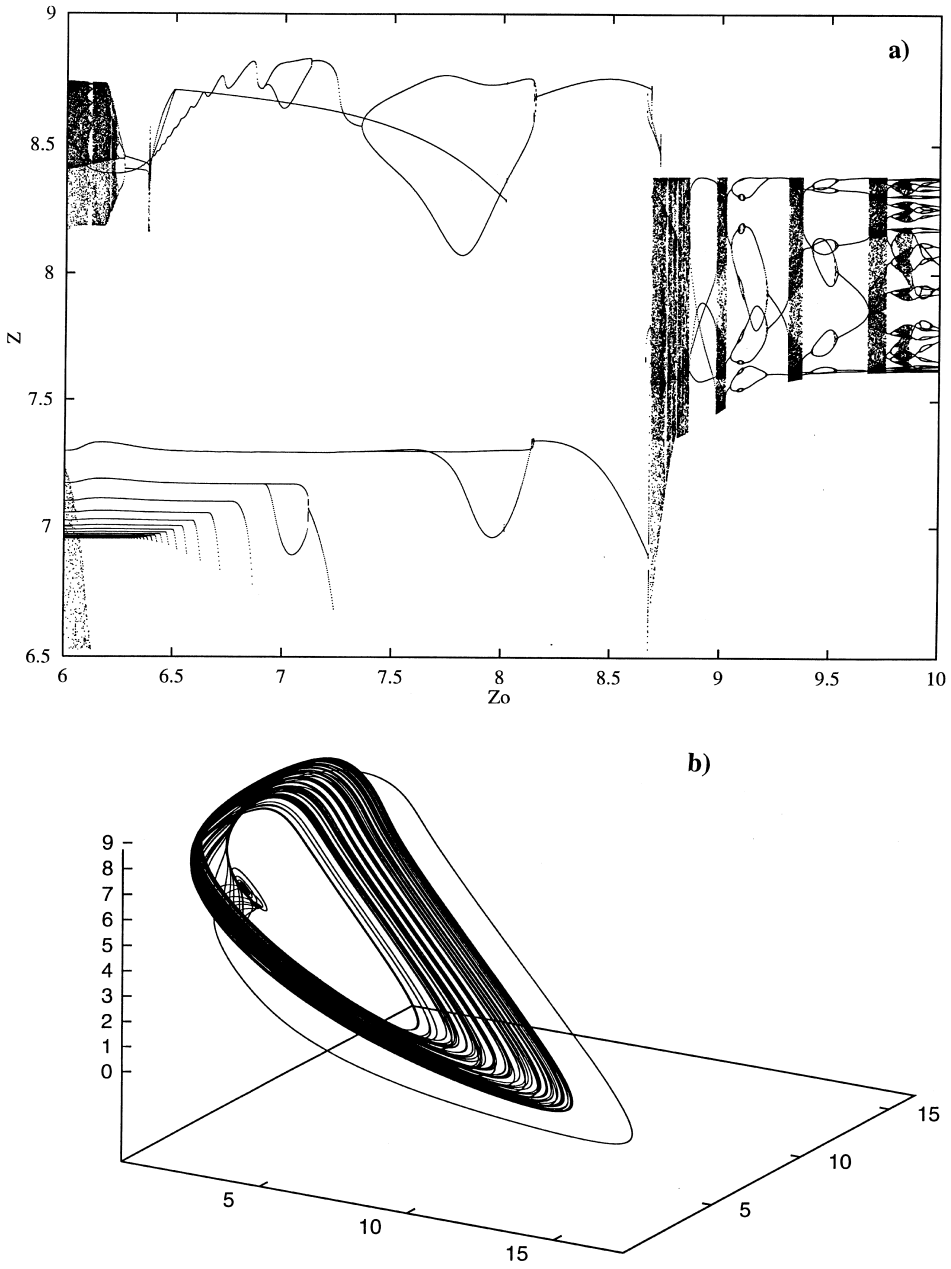

Fig. 10. (a) Backtracked Poincaré section defined by the local maxima of z varying z_0. (b) Three-dimensional x–y–z phase space and (c) amplification. Parameters as in Fig. 7.

different attractors are observed to coexist. In particular, the coexistence of a period-one state with a steady state is observed from $A_2 = 4$ to 5.8; this period-one state coexists with a chaotic attractor from $A_2 = 5.8$ to 6.3 and with a period-3 state for $A_2 \approx 6.4$. Also notice how the x–y–z cell drives the w–v–u cell to a 1:5 cycle as is depicted in Fig. 11b for $A_2 = 1.5$. For the internal variable w, we can see how the concentration increases every time the input flux is open (Fig. 11c). Thus

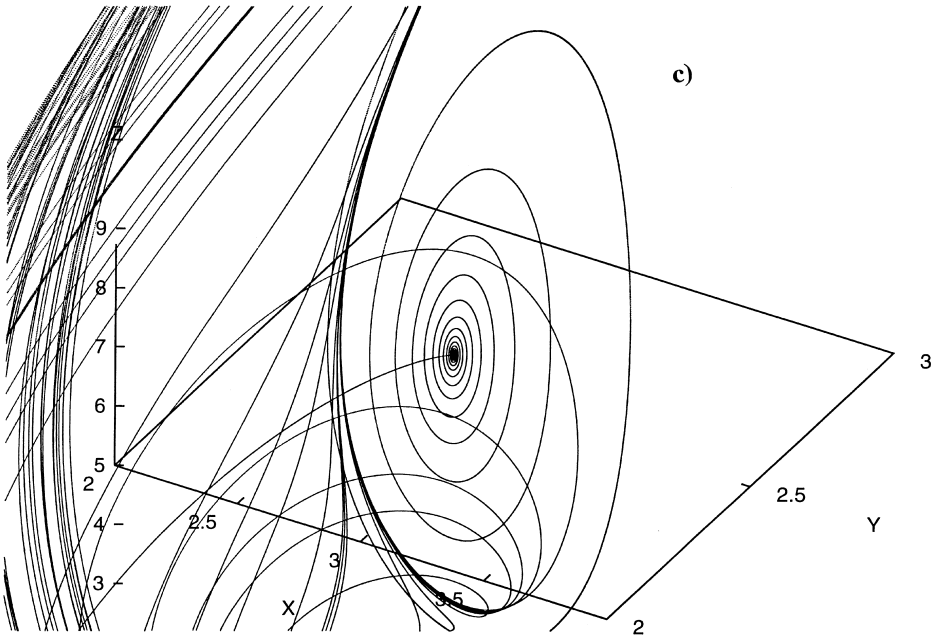

Fig. 10. (*Continued*)

while z shows a periodic behavior, w can show multiples of the z-period.

4. Conclusions

Namely, the coupling parameters were found to be essential in determining the dynamics of the model. In contrast, the non-coupling parameters (those specific to the chemical and mechanistic make-up of each cell) were found to be relatively unimportant. This means that the specific internal mechanism of the oscillators may not be as important in determining the overall system's behavior as we may tend to believe. This is an important observation, since it means that the applicability of the model to physiological systems can be almost independent of the internal mechanisms of chemical messenger production. Without major changes, the model could conceivably be used to model any system within the range of systems outlined in Section 1.

The ability of the simple two-cell model to generate a range of different dynamical behaviors over ranges of the coupling parameters suggests the potential applicability of the coupling function used in our study. There are many other documented endocrine systems involving a circulatory feedback element that the model could be used to analyze. These specific systems are all understood well enough that the model could be formulated to accurately represent them, but there is room for more mechanistic understanding in each case.

The classical example of a circulatory feedback loop is the mutual influence of the oscillating concentrations of dopamine and prolactin. A well-documented cycle of pre-ovulatory surges in these concentrations exists in female mammals [9]. Successfully modelling this loop would prove the usefulness of the model and provide insight into the inherent stability or instability of the documented system of two co-dependent concentrations that can fail as a result of a problem with either hormone.

Another system involving two well-known chemical species is the interaction between the pituitary gland (and hypothalamus) and the thy-

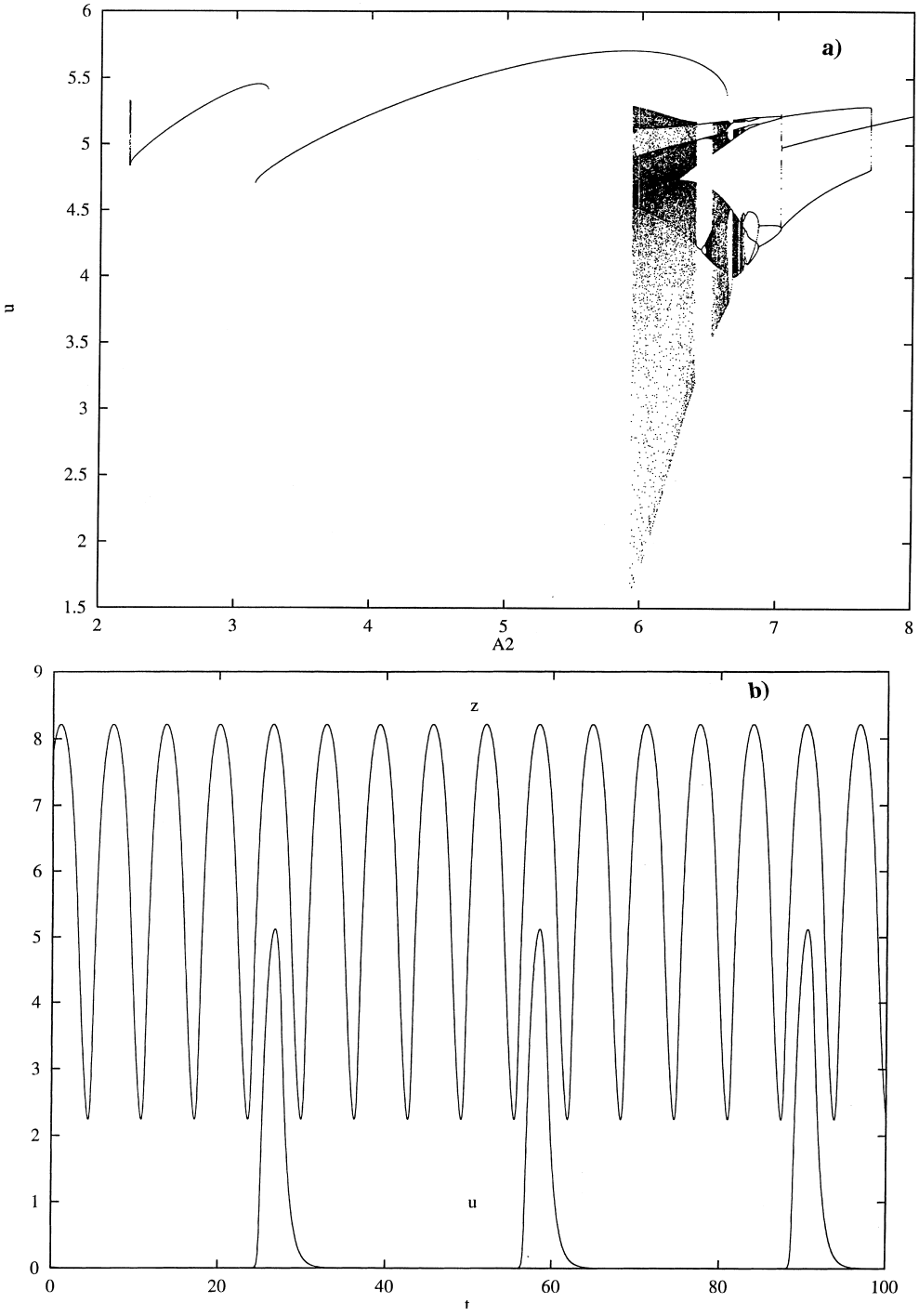

Fig. 11. (a) Backtracked Poincaré section defined by the local maxima of u varying A_2. (b,c) Time series for z, u and w with $A_2 = 1.5$. Parameters as in Fig. 2.

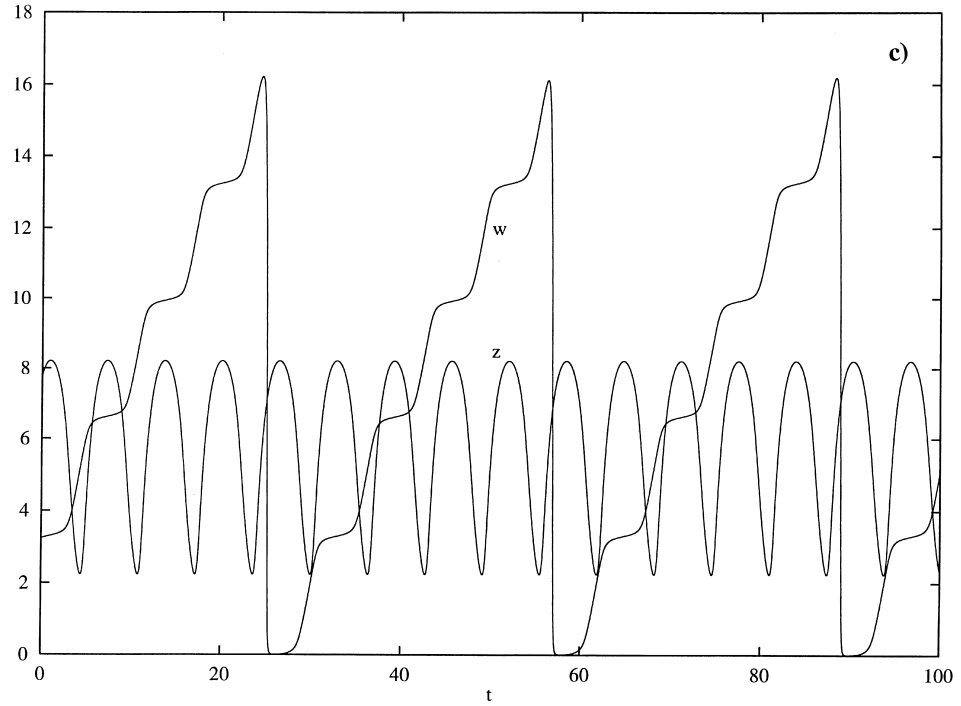

Fig. 11. (*Continued*)

roid. Thyroid stimulating hormone, or TSH, controls the production of thyroxine by the thyroid; thyroxine is the agent that the hypothalamus/pituitary complex uses to determine its output of TSH [7]. Study of this system using established physical features to determine the model's parameters could help to elucidate the mechanism behind the pulsatile release of the two species involved and to aid understanding of thyroid/hormonal ailments.

The central role of pituitary-secreted growth hormone, HGH, in determining liver metabolism has been established but not elucidated [29]. The liver's rate of metabolism and its rhythm in producing certain hormones are both controlled by HGH levels. Some sort of unknown feedback to the hypothalamus/pituitary complex is active, but the mechanism behind the periodicity observed has not been uncovered. Elucidation of this system's workings via a model could help in understanding the entire functioning of the liver, a universally important organ.

The rhythm of liver metabolism also has been documented to be interconnected with the release of gonadal hormones of both sexes. In this case the rhythms have been documented to be characteristically male or female and interconnected with (but not necessarily determined by) gonadal hormone release. Thus, modelling the hypothalamus/pituitary–liver axis as one oscillator (using a hormone characteristic of that system, like HGH) it would be possible to investigate at some depth the connection between that axis and the release of gonadal hormones. This could potentially aid understanding of gonadal hormone-related disorders in a much more global sense than is already possible.

Given the variety of dynamic behaviors observed in this model based on changes in only the coupling parameters, it is not inconceivable that such a coupling could indeed be responsible for many of the release patterns observed in vivo. For example, the observation of hysteresis strengthens the possibility that the model may be

able to shed light on physiological systems that seem to express hysteresis-like behavior in vivo. Being able to understand the extent of hysteresis in a model with the apparent applicability of the two-cell model is a large step in being able to understand similar physical systems that abruptly change behavior and reasons behind these changes in behavior. The observation of hysteresis in this model is an additional feature that, together with the wide range of dynamic behaviors observed, makes a case that this model could provide a fair representation of the important features of real physiological systems.

To prove that the model's behavior is mainly internal-mechanism independent, changes must be made to the internal scheme of the oscillators to verify that the model's behavior will not change. A substitute internal mechanism for the Higgins oscillator mechanism used above could be the templator developed by Peacock-López et al. [30]. Once the model's internal mechanism-independence is studied, more physiologically relevant parameters than the reference values quoted in Table 2 must be used and the behavior of the system characterized. The specific systems described in Section 1 are reasonably documented from which parameter values for use in the model could be gleaned. On the basis of the observations made in this work, the two-cell model is readily applicable to analysis of physiological systems without need for the invasive and still undeveloped analytical techniques available at this time.

Acknowledgements

The authors gratefully acknowledge the support from NSF (CHE93-12160) and the Bronfinan Science Center at Williams College.

References

[1] P.J. Bolt, J. Reprod. Fertil. 24 (1971) 435–438.
[2] L.A. Schotkin, J. Theor. Biol. 43 (1974) 1–14.
[3] L.A. Schotkin, J. Theor. Biol. 43 (1974) 15–28.
[4] T.W. Melnyk, I.W. Richardson, A.A. Simpson, W.R. Smith, Bull. Math. Biol., 38 (1976).
[5] W.J. Bremner, C.A. Paulsen, Horm. Metab. Res. 9 (1977) 1–16.
[6] W.R. Smith, Bull. Math. Biol. 42 (1980) 57–78.
[7] H. Curtisand, N.S. Barnes, Biology, 5th ed., Worth Publishers, New York, 1989.
[8] Y.-X. Li, Pulsatile Hormonal Signaling: A Theoretical Approach, PhD Dissertation, Université Libre de Bruxelles, 1992.
[9] M.H. Johnson, B.J. Everitt, Essential Reproduction, 4th ed., Blackwell Scientific, Oxford, 1995.
[10] J.A. Stamford, J.B. Justice, Anal. Chem. 68 (1996) 359A–363A.
[11] S.H. Strogatz, I. Stewart, Scientific American, Dec., 1993, pp. 102–109.
[12] W.F. Crowley Jr., J.H. Hofler (Ed.), The Episodic Secretion of Hormones, Churchill Livingstone, New York, 1987.
[13] A. Goldbeter, News Physiol. Sci. 3 (1988) 103–105.
[14] Y.-X. Li, A. Goldbeter, Biophys. J. 61 (1992) 161–171.
[15] R. Pool, Science 243 (1989) 604–607.
[16] E. Peacock-López, S. Patel, J. Chem. Phys., 1998, to be submitted.
[17] J. Halloy, Y.-X. Li, J.L. Martiel, B. Wurstier, A. Goldbeter, Phys. Lett. A 151 (1990) 33–36.
[18] M. Marek, I. Schreiber, in: R.J. Field, L. Györgyi (Eds.), Chaos in Chemistry and Biochemistry, World Scientific, Singapore, 1993.
[19] R. Losick, D. Kaiser, Scientific American, Feb., 1997, 68.
[20] S.H. Strogatz, Nonlinear Dynamics and Chaos, Addison-Wesley, Reading, MA, 1994.
[21] R.E. Mirollo, S.H. Strogatz, SIAM J. Appl. Math. 50 (1990) 1645–1662.
[22] T.S. Parker, INSITE, Ver. 4.1, 1990.
[23] D.K. Kahaner, D.D. Barnett, Plotted Solutions of Differential Equations, Ver. 6.00, NIST, Washington, DC, 1989.
[24] O.E. Rössler, Z. Naturforsch. Teil A 31 (1976) 259.
[25] D. Barkley, J. Chem. Phys. 89 (1988) 5547.
[26] F.N. Albahadilly, M. Schnell, J. Chem. Phys. 88 (1988) 4312–4319.
[27] M.J.B. Hauser, L.F. Olsen, J. Am. Chem. Soc. 92 (1996) 2857–2863.
[28] T.V. Bronnikova, W.M. Schaffer, L.F. Olsen, J. Chem. Phys. 105 (1996) 10847–10861.
[29] J.A. Gustafsson, A. Mode, G. Norstedt, P. Shett, Ann. Rev. Physiol. 45 (1983) 51–60.
[30] E. Peacock-Löpez, D.B. Radov, C.S. Flesner, Biophys. Chem. 65 (1997) 171–178.